The Journal of
Chemical Physics

Do not forget the Rydberg orbitals

Cite as: J. Chem. Phys. **156**, 100901 (2022); https://doi.org/10.1063/5.0084574
Submitted: 07 January 2022 • Accepted: 14 February 2022 • Accepted Manuscript Online: 18 February 2022 • Published Online: 08 March 2022

Jack Simons

The Journal of Chemical Physics

PERSPECTIVE

scitation.org/journal/jcp

Do not forget the Rydberg orbitals

Cite as: J. Chem. Phys. 156, 100901 (2022); doi: 10.1063/5.0084574
Submitted: 7 January 2022 • Accepted: 14 February 2022 •
Published Online: 8 March 2022

Jack Simons[a)]

AFFILIATIONS

Henry Eyring Center for Theoretical Chemistry, Department of Chemistry, University of Utah, Salt Lake City, Utah 84112, USA

Note: This paper is part of the JCP Special Topic on Nature of the Chemical Bond.

[a)]**Author to whom correspondence should be addressed:** jack.simons@utah.edu

ABSTRACT

Within any molecule or cluster containing one or more positively charged sites, families of Rydberg orbitals exist. Free electrons can attach directly, and anionic reagents with low electron binding energy can transfer an electron into one of these orbitals to form a neutral Rydberg radical. The possibilities that such a radical could form a covalent bond either to another Rydberg radical or to a radical holding its electron in a conventional valence orbital are considered. This Perspective overviews two roles that Rydberg radicals can play, both of which have important chemical consequences. Attachment of an electron into excited Rydberg orbitals is followed by rapid ($\sim 10^{-6}$ s) relaxation into the lowest-energy Rydberg orbital to form the ground state radical. Although the excited Rydberg species are stable with respect to fragmentation, the ground-state species is usually quite fragile and undergoes homolytic bond cleavage (e.g., $-R_2NH$ dissociates into $-R_2N$ + H or into $-RNH$ + R) by overcoming a very small barrier on its potential energy surface, thus generating reactive radicals (H or R). Here, it is shown that as a result of this fragility, any covalent bonds formed by Rydberg radicals are weak and the molecules they form are susceptible to exothermic fragmentations that involve quite small activation barriers. Another role played by Rydberg species arises when the Coulomb potentials provided by the (one or more) positive site(s) in the molecule stabilize low-energy anti-bonding orbitals (e.g., σ^* orbitals of weak σ bonds or low-lying π^* orbitals) to the extent that electron attachment into these Coulomb-stabilized orbitals is rendered exothermic. In such cases, the overlap of the Rydberg orbitals on the positive site(s) with the σ^* or π^* orbitals allows either a free electron or a weakly bound electron to an anionic reagent that is attracted toward the positive site by its Coulomb force to be guided/transferred into the σ^* or π^* orbital instead. After attaching to such an anti-bonding orbital, bond cleavage occurs again, generating reactive radical species. Because of the large radial extent of Rydberg orbitals, this class of bond cleavage events can occur quite distant from the positively charged group. In this Perspective, several examples of both types of phenomena are given for illustrative purposes.

I. INTRODUCTION

In 1981, Herzberg[1] obtained emission spectra between various electronic states of the ammonium radical NH_4 that led him to introduce the terminology of Rydberg molecules, neutral molecules consisting of a closed-shell cationic core to which an electron is bound to an orbital surrounding the entire molecular framework. Other such molecules include H_3O and H_3, which have one electron in a Rydberg orbital surrounding the closed-shell H_3O^+ or $H_3{}^+$ cation, respectively. The electronic energy level spacings observed seemed to approximately fit the expression for the energy levels of a hydrogen atom but with a modified principal quantum number, which is why these species were called Rydberg molecules. In 1982, Gellene, Cleary, and Porter[2] used a neutralized ion beam method to form NH_4 and determined that this Rydberg molecule has a lifetime with respect to fragmentation of less than 1 μs. It turns out that the excited electronic states of most such Rydberg molecules do not fragment but remain intact at geometries very close to those of their parent cation; only the ground-state Rydberg molecules dissociate (e.g., into NH_3 + H for NH_4). Although the excited states do not fragment, they do undergo relaxation[3–6] to lower-energy electronic states at rates in the $\sim 10^6$ s^{-1} range. These differences in the behaviors of ground and excited Rydberg states will be important later in this Perspective.

It turns out that closed-shell molecular cations can alternatively attach two electrons to one or more of their Rydberg orbitals to form anions. In 1987, Bowen and Eaton[7] carried out photodetachment experiments on the H^- anion solvated by one or more NH_3 molecules. When studying $H^-(NH_3)$, they observed a peak in their data showing an electron binding energy in excess of that of bare H^- as expected (because the NH_3 molecule differentially stabilizes the anion). However, they also found a peak corresponding to an electron binding energy of 0.5 eV, considerably below the 0.72 eV binding energy of bare H^-. Later that same year, Ortiz[8] considered the possibility that a different isomer might be responsible for the 0.5 eV peak and showed using electronic structure calculations that a tetrahedral closed-shell NH_4^+ cation surrounded by two electrons in a Rydberg-like orbital is predicted to have an electron binding energy of 0.42 eV. This isomer of NH_4^- was, thus, termed a double-Rydberg anion. The Ortiz group subsequently studied a wide range of double-Rydberg anions and their publication website[9] provides a wealth of information about these studies. Over the past several years, the Miliordos[10] and Ortiz groups have extended the concepts of Rydberg neutrals and double-Rydberg anions to include much larger species in which one or more electrons are bound to the outer surface of a partially solvated cation in what is essentially a Rydberg-like orbital, and they have termed some of the species solvated electron precursors. Interestingly, in those studies, the pattern of ground- and excited-state orbitals has been found to follow that found in the jellium model rather than in the conventional hydrogenic model. The publication websites[9,10] of these two research groups as well as my own publication websites[11] offer much detail on these novel radicals and ions.

In this Perspective, I attempt to offer perspective on the roles that Rydberg orbitals can play in chemical bonding and reactivity, but by no means, do I try to review all that is known about Rydberg-based species. This Perspective is organized as follows: First, I introduce and illustrate the primary features (shapes, sizes, and electron binding energies) of Rydberg orbitals; these features are common to small Rydberg molecules and anions as well as to Rydberg species arising from a positively charged group within a larger molecule, such as the solvated electron precursors mentioned earlier or a protonated side chain within an polypeptide or protein. Next, I discuss some of our efforts to examine the possibility that Rydberg molecules could use their Rydberg orbitals to form covalent bonds either to other Rydberg molecules or to a conventional valence orbital of another atom or molecule. In this discussion, I examine the putative bonding involving one, two, and three electrons in cationic, neutral, and anionic molecules, respectively. Finally, I introduce examples from my own research in which Rydberg orbitals on charged groups within polypeptides or on the surface of partially solvated cations can facilitate chemical bond cleavages elsewhere in the molecular framework. These examples relate to the so-called electron capture dissociation processes that have proven very useful in the field of mass spectrometry.

II. EXAMPLES OF RYDBERG ORBITALS

The Rydberg orbitals my research has focused on arise when an electron is bound to a positively charged closed-shell cation, such as a protonated amine, protonated alcohol, or protonated sulfide. All such cations exert long-range Coulomb attractive forces on the excess electron that generate a series of bound electronic states whose energies, relative to that of the parent cation, can be approximated by the Rydberg formula

$$E_n \approx \frac{-13.6Z^2 \text{ eV}}{(n-\delta)^2}, \tag{1}$$

which is similar to the energy-level formula for a hydrogenic ion of charge Z. Here, n is the principal quantum number and δ is a so-called quantum defect that accounts approximately for the screening and other effects of the other electrons. Examples resulting from attaching an electron into the ground ($n = 3$) Rydberg orbitals of the NH_4^+ and $H_3C–NH_3^+$ cations are shown in Fig. 1.

The electron in the $n = 3$ NH_4 Rydberg species is bound by ~4 eV, which according to Eq. (1) means that the quantum defect for this state is $\delta = 1.2$. This orbital is assigned the $n = 3$ principal quantum number because NH_4^+ is iso-electronic with the Na^+ cation whose lowest-energy unoccupied orbital is its 3s orbital. One can see that the corresponding orbital for the methyl amine cation has a radial-node character much like that of NH_4^+ but is polarized away from the methyl group as one would expect.

As with the hydrogenic ions in which one electron is bound to a nucleus of charge Z, these closed-shell cations also possess excited electronic states that can be approximately characterized by principal (n) quantum numbers as well as by angular (or point group symmetry) quantum numbers with the orbitals of different angular shapes having different quantum defects because they experience different electronic screening. The orbital shown in Fig. 1 for NH_4 would be called a 3s or $3a_1$ orbital, for example.

In Fig. 2, I show several approximate Rydberg orbitals for NH_4 in which their energies and radial sizes are governed primarily by the n quantum number, while their angular shapes relate to their l quantum number and give rise to differences in their quantum defect parameters δ.

Also shown in Fig. 2 in green (and in red and magenta for the 3s case) are qualitative depictions of a C, N, or O 2p orbital, which is included to give the reader a good idea of how the radial sizes of the Rydberg orbitals compare to the sizes of the valence orbitals of common first-row atoms. These orbitals are placed at distances from the center of the NH_4 moiety near where the Rydberg orbitals have their radial maxima. These size comparisons are important since they relate to the degree to which a Rydberg orbital can overlap, and thus interact, with a valence orbital of a first-row atom. For example, such a first-row valence orbital would be expected to interact less strongly with an $n = 4$ or $n = 5$ Rydberg orbital than with an $n = 3$ Rydberg orbital.

One final example of a Rydberg orbital is shown in Fig. 3 to illustrate that such orbitals also arise on positively charged groups of much larger molecules such as that shown. Here, I show the lowest

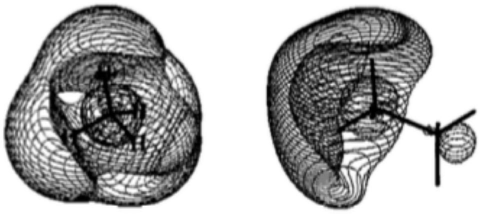

FIG. 1. Lowest-energy orbitals for an electron bound to NH_4^+ (left) and to $H_3C–NH_3^+$ (right). Adapted from Fig. 1 in Ref. 16 with permission from Barrios *et al.*, J. Phys. Chem. A **104**, 10855–10858 (2000). Copyright (2000) American Chemical Society.

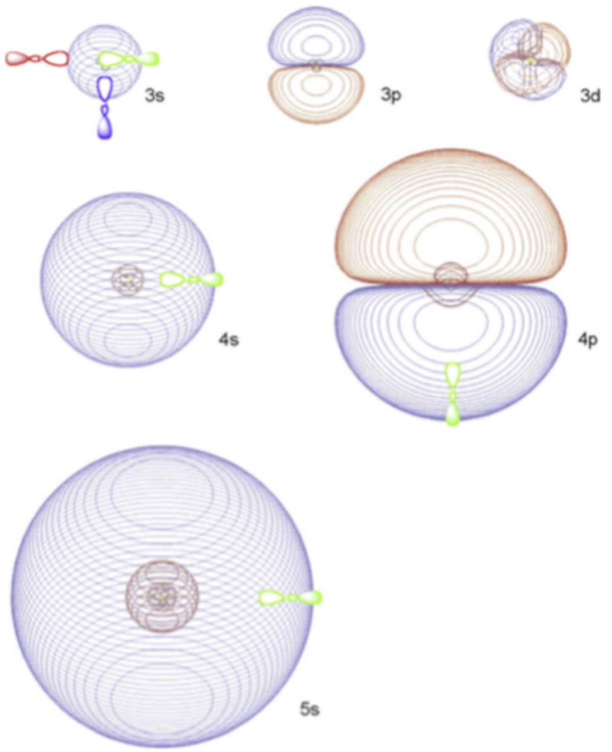

FIG. 2. The approximate *n* and *l* Rydberg orbitals[12] of NH_4 for 3s, 3p, 3d, 4s, 4p, and 5s. In each case, 60% of the total electron density of the orbital is contained within the outermost contour. Reproduced from Fig. 4 in Ref. 23 with permission from J. Simons, J. Am. Chem. Soc. **132**(20), 7074–7085 (2010). Copyright (2010) American Chemical Society.

($3a_1$) Rydberg orbital in green of a large polypeptide (H-Lys-Ala_{20}-SS-Ala_{20}-Lys-H)$^{2+}$ that has been protonated on its two Lys residues' nitrogen atoms.[13] In fact, in Fig. 3, I show only the left half of this doubly charged cation up to the disulfide linkage shown in yellow. The right half has a mirror image shape and also has a Rydberg orbital on its protonated Lys site.

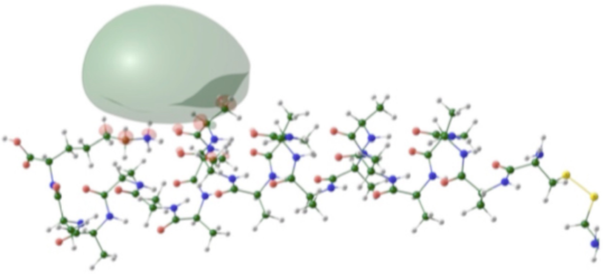

FIG. 3. Ball and stick depiction of the left half of the doubly protonated polypeptide. (H–Lys–Ala_{20}–SS–Ala_{20}–Lys–H)$^{2+}$. Adapted from Fig. 1 in Ref. 24 with permission from Anusiewicz *et al.*, J. Phys. Chem. B **118**, 7892–7901 (2014). Copyright (2014) American Chemical Society.

Later I will discuss how Rydberg orbitals, especially those with higher *n* quantum numbers and thus a larger radial extent, are thought to play a role in directing bond-cleaving electrons or electron-donating anions toward specific bond sites in polypeptides as shown in Fig. 3.

III. CAN ELECTRONS IN RYDBERG ORBITALS FORM BONDS EITHER TO OTHER RYDBERG SPECIES OR TO CONVENTIONAL VALENCE ORBITALS OF OTHER SPECIES?

Several years ago, my colleague Alex Boldyrev and I considered the possibility that two Rydberg fragments could form a covalent bond using their two Rydberg orbitals[14] focusing specifically on bonds between two lowest-energy orbitals. We examined the reaction $NH_4 + NH_4 \rightarrow H_4NNH_4$ and found it to be exothermic by 9 kcal mol^{-1} {at the quadratic configuration interaction including singles and doubles with perturbative treatment of triples [QCISD(T)] level including zero-point energy (ZPE) corrections} and that this geometrical structure was a local minimum on the ground electronic energy surface. Moreover, we saw that the highest occupied molecular orbital (HOMO) of H_4NNH_4 was doubly occupied and was clearly a bonding combination of the two fragments' $3a_1$ Rydberg orbitals as shown in Fig. 4.

However, we also found that H_4NNH_4 was unstable by 93 kcal mol^{-1} [at the QCISD(T)+ZPE level] with respect to the following dissociation:

$$H_4NNH_4 \rightarrow 2NH_3 + H_2. \tag{2}$$

Subsequently, Wright and McKay showed[15] that the transition-state barrier, the reaction shown in Eq. (2) must surmount, is only ~2 kcal mol^{-1}, thus suggesting that the Rydberg-bonded dimer shown in Fig. 4 would likely be very difficult to form and detect and might even undergo spontaneous rearrangement to $2NH_3 + H_2$.

It turns out that the fragility of the Rydberg-bonded species just discussed is likely related to the fragility of the ground states of the constituent Rydberg monomers. Recall I mentioned earlier that the excited electronic Rydberg states of protonated amines, alcohols, and sulfides are geometrically stable but the ground electronic states are only metastable with small energy barriers to fragmentation. For example, the reaction

$$NH_4 \rightarrow NH_3 + H \tag{3}$$

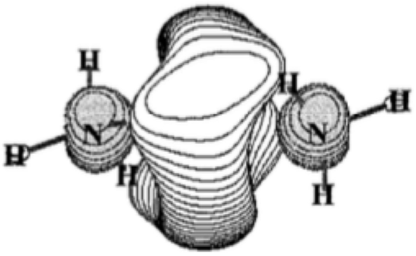

FIG. 4. Doubly occupied HOMO of H_4NNH_4. Adapted from Fig. 1 in Ref. 16 with permission from Barrios *et al.*, J. Phys. Chem. A **104**, 10855–10858 (2000). Copyright (2000) American Chemical Society.

is exothermic by ~2.5 kcal mol^{-1} and has a barrier to surmount of ca. 5–9 kcal mol^{-1} (varying from one theoretical calculation to another). As noted earlier,[2] this results in NH_4 living only ~1 μs before fragmenting. Hence, it appears that ground-state Rydberg monomers are not likely to be long-lived and the rather weak covalent bonds between pairs of them are also likely to exist only fleetingly.

However, there remain several interesting and potentially important features of Rydberg species that I want to discuss relating to the corresponding cations and anions and the possibility of bonding a Rydberg fragment to a conventional valence orbital of another fragment.

First, I want to compare what was found for the neutral H_4NNH_4 putative Rydberg-bonded species and the corresponding cation $H_4NNH_4{}^+$ and anion[16] $H_4NNH_4{}^-$. The anion contains two electrons in a bonding Rydberg orbital and one in the corresponding anti-bonding Rydberg orbital, both of which are shown in Fig. 5.

Not surprisingly, because the excess electron occupies an anti-bonding orbital, the N–N interatomic distance in this anion of 4.22 Å is longer than that in the neutral Rydberg dimer of 3.65 Å shown in Fig. 4, and the dissociation energy for

$$H_4NNH_4{}^- \rightarrow NH_4 + NH_4^-. \tag{4}$$

4 kcal mol^{-1} is smaller than the 9 kcal mol^{-1} cited earlier for the dissociation energy of the corresponding neutral dimer. One more difference worth noting is that the $NH_4{}^-$ anion has been detected experimentally[7] and has been shown to have a larger barrier[17] (~19 kcal mol^{-1}) to fragment into NH_3 + H^- than does the neutral NH_4. Nevertheless, this Rydberg bound dimer anion is also unlikely to be easily formed or detected because of the fragility (especially of the neutral NH_4 unit) just noted.

When examining the corresponding cation and its dissociation[14]

$$H_4NNH_4{}^+ \rightarrow NH_4 + NH_4^+, \tag{5}$$

we found an N–N interatomic distance of 4.5 Å longer than that of the neutral (3.65 Å), which is not surprising since the cation has one fewer electron in the bonding orbital. However, we also found the dissociation energy of the cation to be 20.3 kcal mol^{-1} much larger than that of the anion or neutral. Although these observations and trends might seem unusual, as pointed out in Ref. 14, they are also observed in the alkali metal dimers, cations, and anions, which might not be surprising since NH_4 has a vertical electron detachment energy (~4 eV) and vertical electron affinity (~0.5 eV) that are similar to those of the alkali metals. In other words, the Rydberg neutral, anion, and cation are displaying the same trends in internuclear distances and bond dissociation energies as occurred in Na_2, $Na_2{}^-$, and $Na_2{}^+$.

Although I have discussed mainly Rydberg species arising from the $NH_4{}^+$ closed-shell cation, similar findings have been reported[9] for species based on H_3O^+ and on methyl-substituted variants, such as $(H_3C)_nNH_{4-n}{}^+$ (n = 1–4).

In addition to the possibility that Rydberg monomers might form covalent bonds with other Rydberg monomers, the bonding of a Rydberg monomer to a conventional valence orbital of another species has been examined. In 1999, Boldyrev and I[18] considered the possibility of a bond between the 3s Rydberg orbital of NH_4 and a 2s, 3s, or 4s orbital of Li, Na, or K, respectively. We chose these particular partners for NH_4 because we wanted to optimize the chance of forming a covalent bond, and, as noted earlier, these alkali atoms have ionization potentials and electron affinities similar to those of NH_4. In Fig. 6, I show the local-minimum structures of the corresponding Rydberg–valence bound neutral molecules.

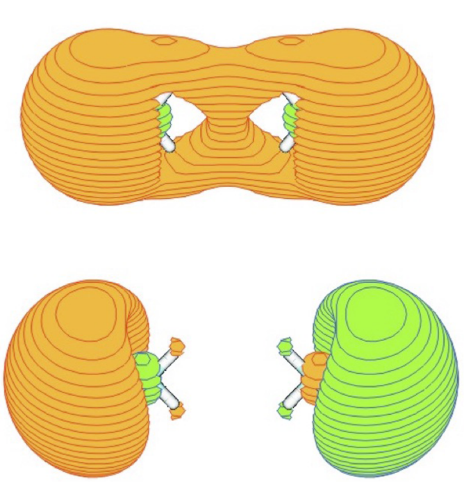

FIG. 5. Bonding (top) and anti-bonding (bottom) Rydberg orbitals of the $H_4NNH_4{}^-$ anion. Reproduced from Fig. 2 in Ref. 16 with permission from Barrios *et al.*, J. Phys. Chem. A **104**, 10855–10858 (2000). Copyright (2000) American Chemical Society.

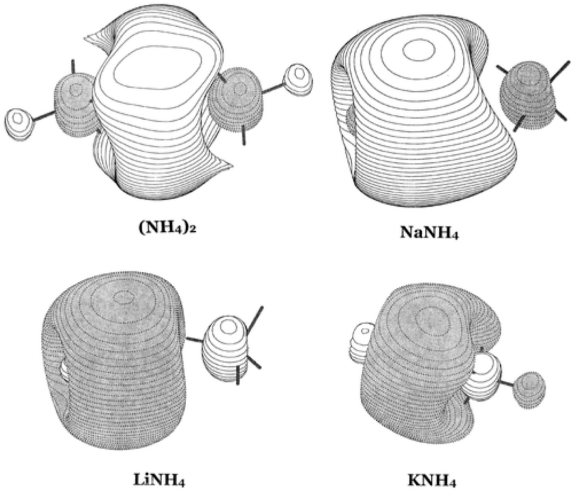

FIG. 6. Local-minimum ground-state geometries and highest occupied molecular orbitals of $(NH_4)_2$ and of the three $(NH_4)X$ molecules (X = Li, Na, K). Reproduced from Fig. 2 of Ref. 18 with permission from A. I. Boldyrev and J. Simons, J. Phys. Chem. A **103**, 3575–3580 (1999). Copyright (1999) American Chemical Society.

The $LiNH_4$ compound was found to be stable with respect to dissociation into Li and NH_4 by 15.9 kcal mol^{-1} and the corresponding bond energies for $NaNH_4$ and KNH_4 turned out to be 12.9 and 9.2 kcal mol^{-1}, respectively. However, again the fragility of the NH_4 moiety comes into play and causes the alternative fragmentation paths

$$XNH_4 \rightarrow HX + NH_3 \quad X = Li, Na, K \tag{6}$$

to be exothermic by 42, 33, and 25 kcal mol^{-1}, respectively, but to have (small) barriers over which these reactions must pass of 1 kcal mol^{-1} for X = Na and 4 kcal mol^{-1} for X = K. For X = Li, $LiNH_4$ is found to have an energy above that of the barrier when zero-point energies are included. Hence, it is found that Rydberg molecules can form weak covalent bonds to conventional valence orbitals, but the intrinsic fragility of the Rydberg monomer causes alternative fragmentation paths to be energetically favored and to have only small barriers to overcome.

In hindsight, which should have been foresight, it is rather clear that the fragility of ground-state Rydberg monomers would make it difficult to form stable covalent bonds either to other Rydberg fragments or to valence orbitals of conventional fragments. In Fig. 7, I illustrate this point by constructing a thermodynamic cycle connecting a Rydberg species consisting of a protonated amine with an electron occupying its 3s Rydberg orbital and another species (denoted X) that is assumed to be capable of forming a covalent bond to the Rydberg species.

In Fig. 7, I have used the electron affinity (EA) of the Cl atom of 3.5 eV and the proton affinity (PA) of the Cl^- ion of 14.4 eV as well as an EA of a typical protonated amine ground-state Rydberg orbital of 4.0 eV and a PA of a typical amine of 5.0 eV to illustrate. Even if I were to consider X to be a much less electronegative species, such as X = CH_3 (the EA of CH_3 is less than 0.1 eV and the PA of CH_3^- is 18.1 eV), the ΔE value (0.1 + 18.1 − 4.0 − 5.0 = 9.2 eV) turns out to highly favor the R_3N + HX species.

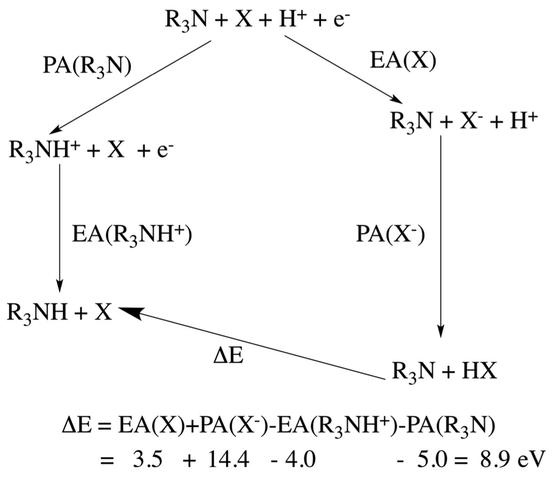

FIG. 7. Thermodynamic cycle diagram connecting $R_3N + X + H^+ + e^-$ to either of the two species that can be formed from these ingredients: R_3N + HX or R_3NH + X. The numerical energies (in eV) relate to X being Cl and R_3N being a typical amine.

Clearly, the amine plus HX products are considerably lower in energy than the Rydberg molecule plus X atom because the proton affinity of the X^- anion is so much larger than that of the amine. This situation likely exists for any candidate fragment X, even if X has a small EA because the PA of X^- is still likely to be large.

Of course, the Rydberg-bound R_3NHX molecule lies a bit (a few kcal mol^{-1}) below that of the R_3NH + X fragments shown in Fig. 7, and the R_3N and HX can hydrogen bond to form a complex $R_3N\cdots HX$ slightly lower than their combined energy by a few kcal mol^{-1}. However, the fact remains that the amine plus HX products will always be favored. This does not mean that the Rydberg molecule R_3NHX cannot exist because, as the earlier discussion showed, there can be barriers on the ground-state energy surface that must be surmounted for these species to convert to the R_3N + HX isomers. However, as the earlier discussion also showed, these barriers are expected to be quite small (a few kcal mol^{-1}).

IV. CAN RYDBERG ORBITALS DO ANYTHING MORE THAN FORM WEAK BONDS THAT MIGHT EXIST ONLY FLEETINGLY?

In Fig. 3, I showed a depiction of a doubly protonated polypeptide containing two lysine units, 40 alanines, and a disulfide linkage $(H–Lys–Ala_{20}–SS–Ala_{20}–Lys–H)^{2+}$. Sequences of contiguous alanines longer than five tend to form α-helices, which combines with the two protonated lysines' Coulomb repulsions to produce a structure similar to that shown in Fig. 8.

In electron-capture dissociation (ECD) mass spectrometry experiments, a positively charged ion, such as that shown in Fig. 3 or Fig. 8, is generated in the gas phase via electrospray from a liquid solution. This gas-phase cation is then allowed to undergo collisions with free electrons of low kinetic energy. For a doubly charged cation, such as that discussed here, capture of a free electron generates a singly charged cation but does so with a variety of outcomes. Some of the parent dications simply attach an electron and remain intact as a monocation; others attach an electron and undergo bond cleavage to generate a neutral fragment and a singly charged cation. For polypeptides, the most commonly observed bond cleavages involve breaking any –S–S– bond or breaking a so-called N–C_α bond along the amino acid backbone, as I will explain now.

The mechanisms by which these ECD-induced bond cleavages occur have been studied over several years,[19,20] after which it has

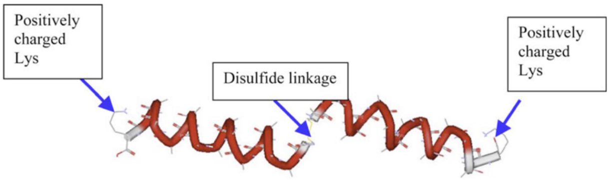

FIG. 8. Quasi-linear structure of polypeptide containing two terminal protonated lysines, a disulfide linkage in the middle, and two series of α-helical alanines. Reproduced from Fig. 2 in Ref. 22 with permission from J. Simons, Chem. Phys. Lett. **484**, 81–95 (2010). Copyright (2010) Elsevier.

been concluded that they involve capture of a free electron into either a disulfide σ* orbital (to cleave the S–S bond) or capture into an amide OCN π* orbital after which a N–C$_\alpha$ bond is cleaved following the path shown in Fig. 9.

A substantial driving force favoring cleavage of the N–C$_\alpha$ bond is the formation of the carbon-centered radical (II in Fig. 9) that then allows for the formation of a C–N π bond (III in Fig. 9) when the N–C$_\alpha$ bond is broken in the II → III step in Fig. 9.

What does this have to do with Rydberg orbitals? It turns out[21] that the direct attachment of an electron to either the SS σ* orbital or to an OCN π* orbital is endothermic by 1 eV or ∼2.5 eV, respectively. The electrons used in the ECD experiments do not have this much kinetic energy, so how and why does such an electron attach to either of these orbitals? The answer to why lies in the Coulomb potentials generated by the two protonated lysine groups of the polypeptide shown in Fig. 3. Each protonated site generates a stabilizing Coulomb energy at the SS or OCN bond site of magnitude

$$C = \frac{14.4\ \text{eV}}{R\ (Å)}, \tag{7}$$

where R is the distance in Å from the positively charged group to the SS or OCN bond. The combination of these two charged groups' stabilization can render attachment to an SS σ* orbital or to an OCN π* orbital exothermic if the SS or OCN unit is close enough. For example, if the distance from each of the two Lys termini is 28 Å, the two stabilizing Coulomb potentials add up to 1 eV, which is sufficient to make attachment of an electron to the SS σ* orbital exothermic. In Fig. 10, I show three plots[13] of the abundances of fragment ions that are formed when a polypeptide as shown in Fig. 3 is fragmented using ECD.

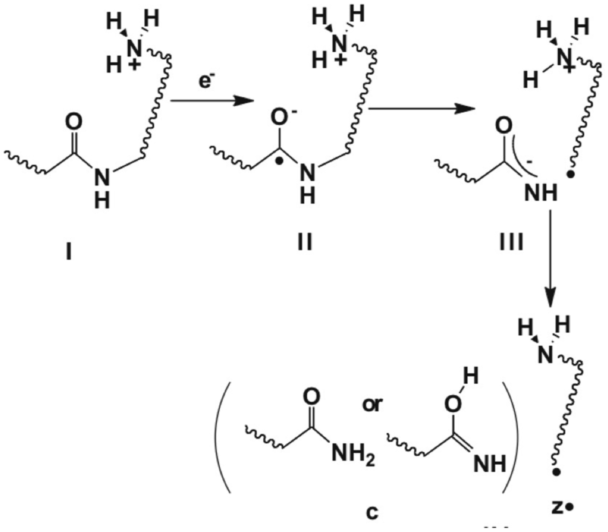

FIG. 9. Adapted from Scheme 1 in Ref. 23 with permission from J. Simons, J. Am. Chem. Soc. **132**(20), 7074–7085 (2010). Copyright (2010) American Chemical Society.

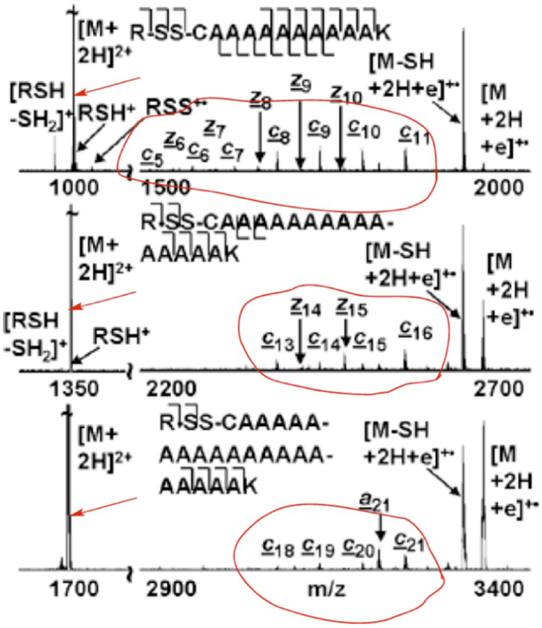

FIG. 10. ECD fragment ion abundances for parent ions of the form shown in Fig. 3 containing 10 (top), 15 (middle), or 20 (bottom) Ala units on each side of the disulfide linkage. Reproduced from Fig. 6 in Ref. 13 with permission from Anusiewicz *et al.*, J. Phys. Chem. B **118**, 7892–7901 (2014). Copyright (2014) American Chemical Society.

The high-intensity peaks on the left indicated by red arrows arise from fragmentation at the S–S linkage; these ions are formed from attachment of a free electron to the SS σ^* orbital. The fact that such an abundant SS bond cleavage occurs even when the polypeptide contains 20 Ala units on each branch is consistent with the Coulomb stabilization model discussed above because even with 20 Ala units, the SS bond is ∼30 Å distant from each of the two protonated Lys groups so this stabilization can exceed 1 eV. Of course, the Lys side chains undergo dynamical movements during which this distance fluctuates a bit, which causes the stabilization energy to also fluctuate, so these estimates of the strength of the Coulomb stabilization must be taken as somewhat imprecise.

The lower intensity peaks labeled c_n and circled in red in Fig. 10 arise from cleavage of N–C$_\alpha$ bonds as described in Fig. 9, where the notation using c_n and z_n for the fragments is introduced. For example, when the polypeptide contains 15 Ala units on each of its two branches (middle plot in Fig. 10), cleavage of the N–C$_\alpha$ bond closest to the protonated site generates the c_{16} fragment, cleavage of the next closest N–C$_\alpha$ bond generates c_{15}, etc., down to c_{13} arising from cleavage of the fourth closest N–C$_\alpha$ bond. Cleavage of N–C$_\alpha$ bonds more distant from the nearest protonated site does not occur because the total Coulomb stabilization potential there is not sufficient to render exothermic attachment of a free electron to the corresponding OCN π^* orbital, which requires ∼2.5 eV as stated earlier.

Although the Coulomb stabilization picture helps explain which bonds will be cleaved, I still need to explain how a free electron is attracted to the SS and OCN bond sites and ends up in an orbital on such a site. Would not a negatively charged electron be accelerated toward one of the protonated lysine sites instead? This is where the Rydberg orbitals come into play. I was able to show[21–24] that free electrons or weakly bound electrons (e.g., by a few tenths of an eV) to a molecular anion donor do indeed move toward a positively charged site (e.g., one of the protonated Lys residues), but as they approach such a site they pass through a series of ground and excited Rydberg orbitals residing on that site. These Rydberg orbitals have angular shapes as explained earlier (see Fig. 2) and they have radial probability distributions that depend primarily on the n quantum number.

In Fig. 11, I show plots of the radial probability distributions [i.e., $\psi^*(r)\psi(r)r^2$] for the 3s through 6s Rydberg orbitals representative of those on a protonated amine. Note that these orbitals' main "peaks" span distances from ~5 Å (for $n = 3$) through more than 20 Å (for $n = 6$).

I showed radial probability distributions only for Rydberg orbitals as high as 6s because my study[24] showed that the cross-sections for electrons (or donor anions) interacting with Rydberg orbitals are comparable for $n = 3$–6 but decrease considerably for higher n values. The overlap of the electron's wave function with the Rydberg orbital decreases with increasing n as suggested in Fig. 2, but the πr^2 factor in the cross-section increases with n with the two factors combining to produce the comparable values for the $n = 3$ to $n = 6$ cross-sections.

In the lower part of Fig. 11, I show a ball and stick representation of one half of the polypeptide of Fig. 3 below which I label (in blue through green) the radial ranges spanned by the $n = 3$ through $n = 6$ Rydberg orbitals. Here, one can see that these orbitals cover space all the way to the SS bond site. In particular, the Rydberg orbitals overlap with the SS σ^* and OCN π^* orbitals along the polypeptide's backbone; the $n = 3$, 4, and 5 orbitals couple with OCN π^* orbitals only and the $n = 6$ orbital couples with the SS σ^* orbital. These orbital interactions are what allows a free electron, while being accelerated toward one of the protonated Lys units and passing through the "cloud" of Rydberg orbitals on that site, to experience attraction to the SS σ^* and OCN π^* orbitals. However, this attraction will be strong enough to allow the electron to enter one of these anti-bonding orbitals only if the total Coulomb stabilization at that orbital site is sufficient (1 eV for SS; ~2.5 eV for OCN), as explained earlier.

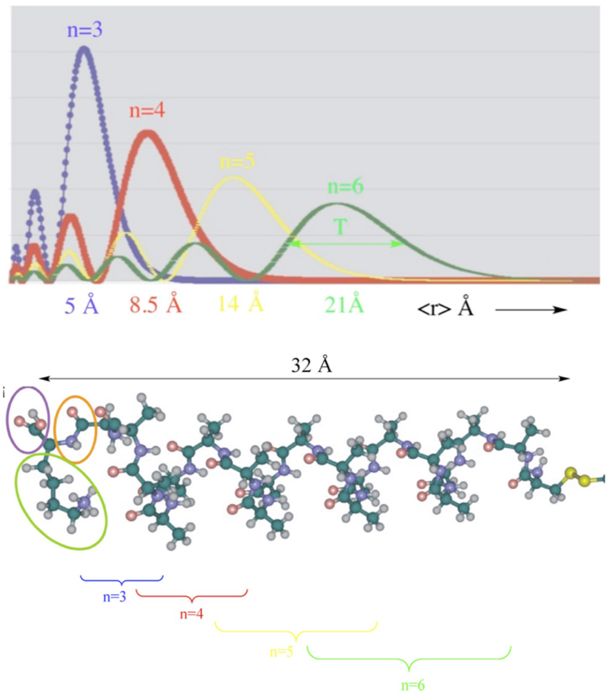

FIG. 11. Reproduced from Fig. 4 (top) and Fig. 5 (bottom) in Ref. 13 with permission from Anusiewicz *et al*., J. Phys. Chem. B **118**, 7892–7901 (2014). Copyright (2014) American Chemical Society.

Hence, the family of Rydberg orbitals surrounding positively charged sites on the polypeptide provide a path by which free electrons can attach to the SS σ^* and OCN π^* orbitals and thus cleave disulfide or N–C$_\alpha$ bonds in the ECD experiment. I will now provide another example of the roles played by Rydberg orbitals and Coulomb stabilization.

In ECD experiments[24,25] using $[\mathrm{Ca(H_2O)}_n]^{2+}$ as parent ions, it was found that two families of fragment ions can be formed. One family contains fragment ions $[\mathrm{Ca(H_2O)}_{n-k}]^{1+}$ that have simply attached a free electron and subsequently lost some water molecules (k in this example). The other family contains ions $[\mathrm{CaOH(H_2O)}_{n-m}]^{1+}$ that have lost some water molecules but have also had one water molecule dissociate to generate a CaOH unit (and lose an H atom in addition to the lost water molecules). In Fig. 12, I show the mass spectral intensity profile for the case in which $[\mathrm{Ca(H_2O)_{24}}]^{2+}$ was the parent ion. Here, one sees fragment ions $[\mathrm{Ca(H_2O)_{14}}]^{1+}$ resulting from the loss of ten water molecules as well as several fragment ions $[\mathrm{CaOH(H_2O)_{14}}]^{1+}$, $[\mathrm{CaOH(H_2O)_{13}}]^{1+}$, and $[\mathrm{CaOH(H_2O)_{12}}]^{1+}$ arising from loss of water molecules and splitting one water molecule to generate the CaOH unit.

It turns out[24,25] that the capture of a free electron by the doubly charged parent ion $[\mathrm{Ca(H_2O)}_n]^{2+}$ is exothermic enough (~5 eV) to allow ten water molecules to be ejected from the cluster, so it

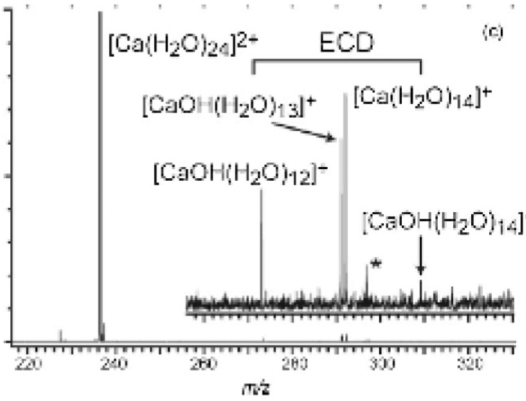

FIG. 12. Reproduced from Fig. 2 in Ref. 26 with permission from D. Neff and J. Simons, Int. J. Mass Spectrom. **277**, 166–174 (2008). Copyright (2008) Elsevier.

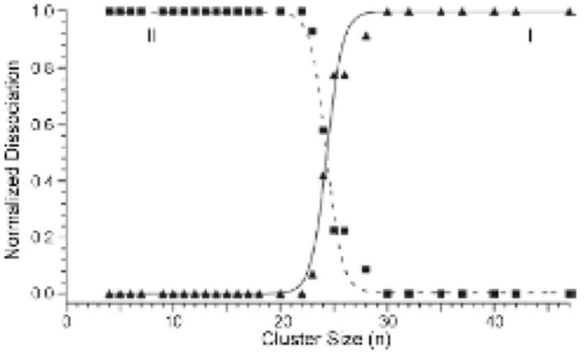

FIG. 13. Reproduced from Fig. 3 in Ref. 26 with permission from D. Neff and J. Simons, Int. J. Mass Spectrom. **277**, 166–174 (2008). Copyright (2008) Elsevier.

is easy to understand the origin of that class of fragment ions. To understand how the $[CaOH(H_2O)_{n-m}]^{1+}$ ions are formed, I note that it is believed that the Ca^{2+} cation's first hydration shell contains six water molecules, while its second hydration shell contains an additional ~20 water molecules. In Fig. 13, I show plots of the fraction of ions that have only lost water molecules (triangles) and those that have formed the CaOH unit and lost water molecules (squares) as functions of the number n of water molecules in the parent dication $[Ca(H_2O)_n]^{2+}$.

Clearly, one can see that the tendency to form fragment ions containing the CaOH unit changes rapidly as the cluster size increases from near unity to near zero at a critical cluster size of ~25 water molecules.

In 2008, Neff and I examined[26] a similar system with Mg^{2+} replacing Ca^{2+}. In this case, the first hydration shell is thought to contain six water molecules and the second shell to add another ~12. In Fig. 14, I show on the left the lowest-energy Rydberg orbital surrounding an intact closed-shell $[Mg(H_2O)_6]^{2+}$ cation. In the middle, I show the corresponding Rydberg orbital for the same system but with one more water molecule placed at a distance from the Mg^{2+} ion representative of the location of a second hydration shell molecule. On the right, I show the O–H σ^* orbital of a first-shell water molecule; the Rydberg orbital has been removed to clarify the appearance of this anti-bonding orbital.

The key to understanding the changes in fragment ion distributions shown in Fig. 13 is to appreciate the role of the Rydberg orbital of the parent dication and the influence of the Coulomb potential generated by the Ca^{2+} or Mg^{2+} ion on the surrounding water molecules. As noted earlier, attachment of a free electron to the Rydberg orbital in the Ca^{2+} case is exothermic by ca. 5 eV; this is enough energy to subsequently "boil off" up to ten water molecules from, for example, $[Ca(H_2O)_{24}]^{2+}$. The Coulomb potential [Eq. (7)] generated by the central dication will be strong enough to render exothermic addition of a free electron to a solvent water molecule's OH σ^* orbital if the water molecule is close enough. It is through the latter process that one H_2O molecule dissociates to form an H atom and an OH^- ion, which, in turn, generates the $[CaOH]^{1+}$ or $[MgOH]^{1+}$ ion that occurs in the second family of fragment ions. How close does a water molecule have to be to the central dication to make this possible? One has to have [n.b., in Eq. (7), $Z = 2$ in this case]

$$\frac{28.8\ \text{eV}}{R\ (\text{Å})} > EA_{Rydberg} - EA_{\text{OH}} + D_0(\text{O}-\text{H}), \tag{8}$$

where $EA_{Rydberg}$ is the energy gained when a free electron attaches to the Rydberg orbital (~5 eV), EA_{OH} is the electron affinity of the OH radical (~2 eV), and D_0(O–H) is the energy needed to homolytically cleave an OH bond in a water molecule (~5 eV). This condition requires R to be 3.35 Å or less. For both $[Ca(H_2O)_n]^{2+}$ and $[Mg(H_2O)_n]^{2+}$, the first-shell water molecules reside within this distance, but the second- and higher-shell molecules do not. This suggests that a first-shell water molecule must be accessed by the ECD electron to form the CaOH or MgOH unit arising in the second class of fragment ions.

FIG. 14. Adapted from Figs. 5, 7, and 8 in Ref. 26 with permission from D. Neff and J. Simons, Int. J. Mass Spectrom. **277**, 166–174 (2008). Copyright (2008) Elsevier.

In summary, the fragment ions found when the parent cations discussed above are studied using ECD can be explained as being formed (a) by direct attachment of a free electron to the parent dication's Rydberg orbital followed by radiationless relaxation that boils water molecules off or (b) by attachment of a free electron to the Rydberg orbital followed by transfer of the excess electron to the anti-bonding O–H σ^* orbital of a first-shell water molecule to form the OH^- anion and a neutral H atom (which is eventually ejected). For $[Ca(H_2O)_n]^{2+}$ with $n > {\sim}25$ (see Fig. 13) and for $[Mg(H_2O)_n]^{2+}$ with $n > {\sim}17$, the second hydration shell is full, so there exists no pathway by which the excess electron can access a first-shell water molecule's O–H σ^* orbital. For lower n values, the second hydration shell is not full so one or more first-shell water molecules have O–H σ^* orbitals accessible to attachment by the extra electron. Finally, only the first-shell water molecules can undergo the second fragmentation process because only they are close enough to the central dication to experience sufficient Coulomb stabilization.

One might expect that the effects of Coulomb stabilization key in both the peptide and water clustered ions discussed above would be diminished by dielectric screening, but this is not the case. Full dielectric screening (e.g., in which the Coulomb interaction would be reduced by a factor of $1/\varepsilon$, where ε is the bulk static dielectric constant) occurs only when the positively charged group and the electron (or anion donor) are fully solvated and widely separated from one another.[27] For the gas-phase species discussed here, this is certainly not the case. Moreover, even when the system composed of a positively charged unit and a free electron or anion donor are surrounded by bulk solvent but are relatively close to one another, their Coulomb interaction is only partly screened.

V. SUMMARY

In this Perspective, I hope to have provided perspective about how the presence of positively charged groups within a molecule can, through their Coulomb potentials and the Rydberg orbitals that surround them, give rise to bond cleavages both within the charged unit and elsewhere in the molecule, including quite far away. Whenever such a closed-shell charged group exists and either a free electron (e.g., as in the ECD experiments discussed here or via photon-induced from another location) or an anionic electron donor is operative, it is important to consider two possibilities.

First, it is possible for an electron to attach directly to one of the Rydberg orbitals on the positive site. If attached into an excited Rydberg orbital, relaxation to the ground-state orbital within $\sim 10^{-6}$ s will occur after which one of the bonds within the previously charged site will most likely homolytically cleave (because of the very small activation barrier it needs to surmount). For example, at a $-NR_2H^+$ site, electron attachment could lead to cleavage to generate either $-NR_2$ + H or $-NRH$ + R. These reactions generate free radicals (H or R in these examples) that can subsequently undergo reactions elsewhere within the molecule or with nearby molecules. References 3 and 9–11 offer much more information about these species and processes.

The second possibility involves the positively charged site(s) inducing Coulomb stabilization of anti-bonding orbitals elsewhere in the molecule and allowing Rydberg orbitals on the positive site(s) to facilitate electron attachment to one of these anti-bonding orbitals by overlapping/coupling with that orbital. Low-energy anti-bonding orbitals (e.g., σ^* orbitals of weak σ bonds or low-energy π^* orbitals) are the most susceptible to this process. Because the Rydberg orbitals can span large distances as can the Coulomb stabilization, this class of electron attachments (either by free electrons or from an anion donor) can take place far from the charged site(s). After electron attachment to the anti-bonding orbital, bond cleavage can occur, which, as in the first case, generates a free radical that can induce other reactions elsewhere. References 11 and 14–26 and the websites of Williams[28] and Turecek[29] provide much more information about this kind of process.

Hence, even though species generated by attaching an electron to a Rydberg orbital of a closed-shell positively charged site are fragile in the sense explained earlier (i.e., they undergo rather prompt dissociation in their ground states), it is important for the chemist to not forget about the on-site and potentially distant bond cleavages that these charged units and their Rydberg orbitals can generate.

AUTHOR DECLARATIONS

Conflict of Interest

The author has no conflicts to disclose.

DATA AVAILABILITY

Data sharing is not applicable to this article as no new data were created or analyzed in this study.

REFERENCES

[1] G. Herzberg, Faraday Discuss. Chem. Soc. **71**, 165–173 (1981).

[2] G. I. Gellene, D. A. Cleary, and R. F. Porter, J. Chem. Phys. **77**, 3471–3477 (1982).

[3] F. Turecek and P. J. Reid, Int. J. Mass Spectrom. **222**, 49–61 (2003).

[4] V. Q. Nguyen, M. Sadilek, J. Ferrier, A. J. Frank, and F. Tureček, J. Phys. Chem. A **101**, 3789–3799 (1997).

[5] M. Sadílek and F. Tureček, J. Phys. Chem. **100**, 9610–9614 (1996).

[6] M. Sadílek and F. Tureček, Chem. Phys. Lett. **263**, 203–207 (1996).

[7] K. H. Bowen and J. G. Eaton, in *The Structure of Small Molecules and Ions*, edited by R. Naaman and Z. Varger (Plenum Press, New York, 1987), p. 147.

[8] J. V. Ortiz, J. Chem. Phys. **87**, 3557–3562 (1987).

[9] See http://www.auburn.edu/cosam/faculty/chemistry/ortiz/research/info_pubs.html.

[10] See http://www.auburn.edu/cosam/faculty/chemistry/miliordos/my_lab/page4.htm.

[11] See http://simons.hec.utah.edu/publications.html.

[12] J. Simons, J. Chem. Phys. **117**, 9124–9132 (2002).

[13] I. Anusiewicz, P. Skurski, and J. Simons, J. Phys. Chem. B **118**, 7892–7901 (2014).

[14] A. I. Boldyrev and J. Simons, J. Phys. Chem. **96**, 8840–8843 (1992).

[15] J. S. Wright and D. McKay, J. Phys. Chem. **100**, 7392–7397 (1996).

[16] R. Barrios, P. Skurski, and J. Simons, J. Phys. Chem. A **104**, 10855–10858 (2000).

[17] H. Cardy, C. Larrieu, and A. Dargelos, Chem. Phys. Lett. **131**, 507–512 (1986).

[18] A. I. Boldyrev and J. Simons, J. Phys. Chem. A **103**, 3575–3580 (1999).

[19] F. Turecek and R. R. Julian, Chem. Rev. **113**, 6691–6733 (2013).

[20] E. A. Syrstad and F. Turecček, J. Am. Soc. Mass Spectrom. **16**, 208–224 (2005).

[21] I. Anusiewicz, J. Berdys-Kochanska, and J. Simons, J. Phys. Chem. A **109**, 5801–5813 (2005).

[22] J. Simons, Chem. Phys. Lett. **484**, 81–95 (2010).

[23] J. Simons, J. Am. Chem. Soc. **132**(20), 7074–7085 (2010).

[24] R. D. Lieb, W. A. Donald, M. F. Bush, J. T. O'Brien, and E. R. Williams, J. Am. Soc. Mass Spectrom. **18**, 1217–1231 (2007).

[25] R. D. Lieb, W. A. Donald, M. F. Bush, J. T. O'Brien, and E. R. Williams, J. Am. Chem. Soc. **129**, 4894–4895 (2007).

[26] D. Neff and J. Simons, Int. J. Mass Spectrom. **277**, 166–174 (2008).

[27] A. Warshel, S. T. Russell, and A. K. Churg, "Macroscopic models for studies of electrostatic interactions in proteins: Limitations and applicability," Proc. Natl. Acad. Sci. U. S. A. **81**, 4785–4789 (1984).

[28] See http://www.cchem.berkeley.edu/erwgrp/index.html.

[29] See https://sites.uw.edu/ftlab/.